

UNCLASSIFIED

AD NUMBER

AD007616

LIMITATION CHANGES

TO:

Approved for public release; distribution is unlimited.

FROM:

Distribution authorized to DoD only; Administrative/Operational Use; DEC 1952. Other requests shall be referred to Office of Naval Research, Arlington, VA 22203. Pre-dates formal DoD distribution statements. Treat as DoD only.

AUTHORITY

ONR ltr dtd 26 Oct 1977

THIS PAGE IS UNCLASSIFIED

UNCLASSIFIED

AD _____

DEFENSE DOCUMENTATION CENTER

FOR

SCIENTIFIC AND TECHNICAL INFORMATION

CAMERON STATION ALEXANDRIA, VIRGINIA

DOWNGRADED AT 3 YEAR INTERVALS:
DECLASSIFIED AFTER 12 YEARS
DCD DIR 5200.10



UNCLASSIFIED

THIS REPORT HAS BEEN DECLASSIFIED
AND CLEARED FOR PUBLIC RELEASE.

DISTRIBUTION A
APPROVED FOR PUBLIC RELEASE;
DISTRIBUTION UNLIMITED.

AD No. 7616
NOTED

CALIFORNIA INSTITUTE OF TECHNOLOGY
Hydrodynamics Laboratory

EVALUATION OF THE INTEGRALS
OCCURRING IN THE CAVITY THEORY
OF PLESSET AND SHAFFER

Byrne Perry

Report No. 21-11

OFFICE OF NAVAL RESEARCH

Contracts N6onr-24420 (NR 062-059) and N6onr-24424 (NR 234-001)

Department of the Navy
Office of Naval Research
Contract N6onr-24420
Contract N6onr-24424

THE EVALUATION OF INTEGRALS OCCURRING IN THE
CAVITY THEORY OF PLESSET AND SHAFFER

Byrne Perry

Hydrodynamics Laboratory
California Institute of Technology
Pasadena, California

Project Supervisor:
J. P. O'Neill

Approved by:
M. S. Plesset

Report No. 21-11
December, 1952

CONTENTS

	Page
Abstract	iii
Symbols	iv
Introduction	1
Theory of Plesset and Shaffer	2
Pressure Distribution	4
Drag in Two Dimensions	7
Drag in Three Dimensions	9
Cavity Shape in Two Dimensions	10
Expansion in Series of $\sin \lambda \psi$ and $\cos \lambda \psi$	11
Evaluation of Integrals $R(\alpha, \beta)$ and $S(\alpha, \beta)$	13
Approximations for Low Cavitation Numbers	15
References	21
Tables	22

ABSTRACT

The integrals which determine the physical parameters of chief interest in the cavity theory of Plesset and Shaffer are systematically considered. Their numerical integrations are shown to be very accurate with the exception of the values for cavity size at low cavitation numbers. Where necessary, these values have been replaced with accurate tabulations computed by use of suitable series expansions; also, asymptotic formulas valid for low cavitation numbers are presented.

SYMBOLS

<p>a, length of wedge face (Fig. 1).</p> <p>b, parameter fixing scale of problem.</p> <p>C_D, two-dimensional drag coefficient: $C_D = D / \frac{1}{2} \rho v_\infty^2 d.$</p> <p>$C_{3D}$, three-dimensional drag coefficient: $C_{3D} = \frac{1}{2} \rho v_\infty^2 \left(\frac{\pi}{4} d^2 \right).$</p> <p>$C_p$, pressure coefficient: $C_p = (p - p_\infty) / \frac{1}{2} \rho v_\infty^2.$</p> <p>D, drag force.</p> <p>d, width of base of wedge or cone.</p> <p>d_m, maximum width of cavity.</p> <p>g_n, Fourier coefficient. See Eq. (43).</p> <p>h_o, Fourier coefficient. See Eq. (44).</p> <p>h_n, Fourier coefficient. See Eq. (44).</p> <p>I_n, integral defined by Eq. (45).</p> <p>ΔI, estimate of $(I_{n+1} - I_n)$ when $n \rightarrow 6$.</p> <p>J_n, integral defined by Eq. (46).</p> <p>l, length of cavity (Fig. 6).</p> <p>P, $P(\phi, \beta) = 1 - \left[\frac{1 - \sin \phi}{\cos \phi} \right]^{\frac{4\beta}{\pi}}.$</p> <p>p, pressure at any point.</p> <p>P_k, pressure in the cavity.</p> <p>P_∞, pressure at infinity.</p> <p>Q, $Q(\phi, \beta) = \cos \phi \sin \phi \left[\frac{1 + \sin \phi}{\cos \phi} \right]^{\frac{2\beta}{\pi}}$</p> <p>R, integral defined by Eq. (49).</p> <p>S, integral defined by Eq. (50).</p>	<p>t, complex variable. See Eq. (2).</p> <p>v_∞, velocity at infinity.</p> <p>v_o, ratio of velocity at infinity to that on cavity wall.</p> <p>W, complex potential: $W = U + iV$.</p> <p>\bar{x}, abscissa of maximum cavity width (Fig. 1).</p> <p>\bar{y}, vertical distance from A to I (Fig. 1).</p> <p>dY, dimensionless coordinate defined by Eq. (9).</p> <p>Y, integral defined by Eq. (13).</p> <p>z, complex physical coordinate: $z = x + iy.$</p> <p>α, parameter related to cavitation number by Eq. (4).</p> <p>β, wedge or cone half-angle.</p> <p>Δ, $= \Delta(\alpha, \phi) = (1 - \sin^2 \alpha \sin^2 \phi)^{-3/2}.$</p> <p>$\Delta'$, $= \Delta'(\phi, \alpha) = (1 - \cos^2 \alpha \cos^2 \phi)^{-3/2}.$</p> <p>$\zeta$, dimensionless complex velocity, normalized to unity on AIA'.</p> <p>η, complex variable.</p> <p>θ, $\arg \zeta.$</p> <p>λ, $\lambda = 2\beta/\pi.$</p> <p>ρ, fluid density.</p> <p>σ, cavitation number.</p> <p>ϕ, parameter (real).</p> <p>ψ, $\arg \eta.$</p>
--	--

Note: The notation used for elliptic integrals E, K, etc., is that of Ref. 8.

INTRODUCTION

The usual criticism of the classical wake theory¹ is that it fails to account for the large suction pressure on the downstream side of the body. This objection is in part overcome by the theory of Riabouchinsky², who constructed a mathematical model of the wake flow around a flat plate by placing an image plate downstream with a wake region at constant underpressure in between. Whatever the eventual usefulness of his theory for wake flows may be, it is now certain that such a model is very helpful in cavity flow analysis. Here the underpressure in the cavity is specified dimensionlessly by the cavitation number σ , defined by

$$\sigma = \frac{p_{\infty} - p_k}{\frac{1}{2} \rho v_{\infty}^2} \quad (1)$$

where p_{∞} and v_{∞} are the pressure and velocity at infinity, p_k is the pressure in the cavity, and ρ is the liquid density. Riabouchinsky's model may also be

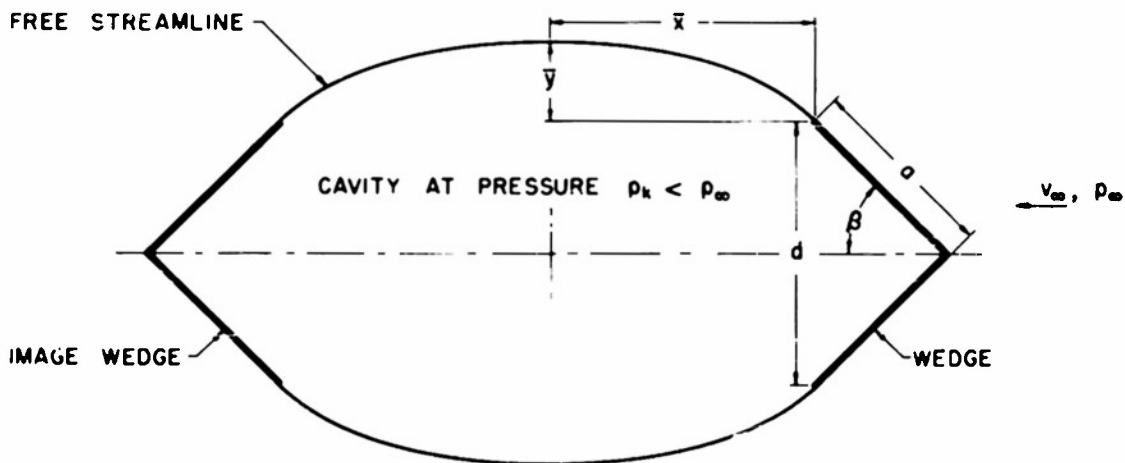


Fig. 1. The cavity flow about a symmetrical wedge according to Plesset and Shaffer.

useful in finding two-dimensional strut shapes which have small tendency to cavitate, since the cavity or wake may equally well be supposed to represent a body with constant pressure over most of its surface. In any event, Plesset and Shaffer^{3,4,5} extended Riabouchinsky's theory to include symmetrical wedges (Fig. 1) with a view to applying the results to cavity flow problems.* Their work

* It should be remarked that many of Plesset and Shaffer's results have been given in an interesting report by J. W. Fisher⁷, which has only recently been declassified.

may also be regarded as an extension of the results of Bobyleff⁶, who considered the symmetrical wedge with an infinite wake, which corresponds to the cavity flow with zero cavitation number.

The present report is concerned for the most part with the evaluation of certain integrals in terms of which the cavity parameters of interest in Plesset and Shaffer's theory can be represented. They computed these integrals numerically, in most cases with high accuracy, thereby obtaining reliable values for the drag, which was the chief concern in their investigations. The cavity dimensions at high cavitation numbers were also accurately tabulated; the values for low cavitation numbers, however, are somewhat in error.

Since there is much emphasis at present on applications where the cavitation number is small, Professor Plesset suggested that the cavity dimensions might be computed analytically in this special case. Such calculations have indeed proved feasible so that it is now possible to evaluate the drag and cavity dimensions with reasonable accuracy for any case likely to occur in practice. The following pages give a summary of these calculations.

THEORY OF PLESSET AND SHAFFER

The theory of Plesset and Shaffer, which uses well-known methods of conformal mapping to solve the two-dimensional potential flow problem, will be outlined here for reference only. For a more complete exposition, as well as for remarks on the comparison with experiment, the reader should consult the original report^{3,4,5}.

In Fig. 2 is shown the hodograph- or ζ -plane* which can be constructed by inspection of the velocity along the streamline KCAIA'C'K' in the physical- or z-plane. Also indicated is the plane of complex potential $W = U + iV$, which can be drawn immediately. The mathematical problem can now be solved by conformally mapping the ζ -plane onto the W-plane. The mappings which effect this are

$$\eta \frac{z}{b} = \zeta, \quad (2a)$$

$$t = \frac{i}{2} \left[\frac{1}{\eta} - \eta \right], \quad (2b)$$

$$W = \frac{b t}{(\tan^2 \alpha + t^2)^{1/2}}, \quad (2c)$$

* Plesset and Shaffer normalize the velocity to unity on the free streamline AIA', so that ζ is the ratio of the reflected velocity to the velocity on AIA'. Similarly, the potential defined by Plesset and Shaffer has the dimensions of length, rather than length times velocity.

where η and t are auxiliary variables as shown in Fig. 2. These mappings, along with the fundamental property of the complex potential,

$$\frac{dW}{dz} = \zeta, \quad (3)$$

enable one in principle at least to calculate the potential at any point z .

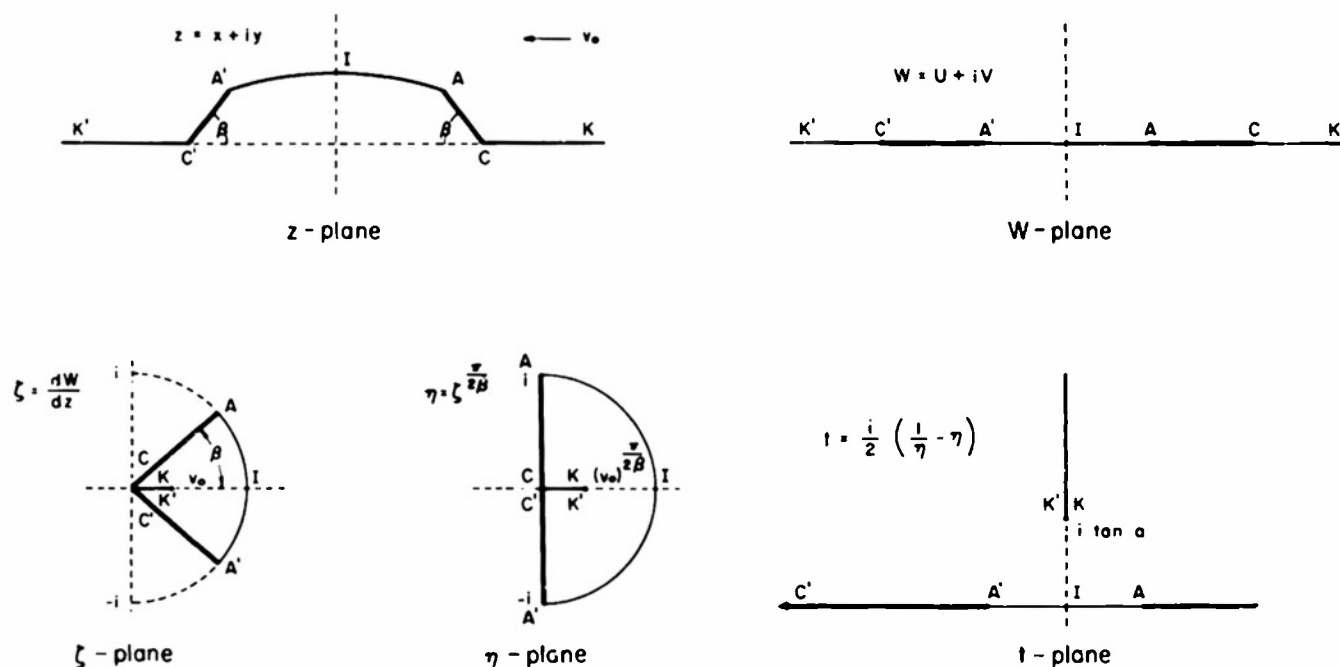


Fig. 2. The mappings corresponding to Eq. (2 a b c).

The parameter b fixes the scale of the problem; since all results of the theory are presented in dimensionless form, it disappears in the final equations. The parameter a may be related to v_0 by calculating $|\zeta|$ at K in terms of W . From Eq. (2 a b c) one finds that

$$v_0 \frac{\pi}{2\beta} = \frac{1 - \sin \alpha}{\cos \alpha}.$$

But application of Bernoulli's equation along the streamline $KCAIA'$ in conjunction with Eq. (1) leads to

$$1 + \sigma = \frac{1}{v_0^2}$$

and hence

$$1 + \sigma = \left[\frac{1 + \sin \alpha}{\cos \alpha} \right]^{\frac{2\beta}{\pi}} \quad (4)$$

Since it is convenient to calculate the other parameters in terms of σ , Table 1 has been constructed for corresponding values of σ from Eq. (4).

The set of equations (2abc) and (3) enable one to calculate the value of the velocity at any point in the z -plane, and the shape of any streamline, including the cavity wall AIA' . Plesset and Shaffer calculated only the quantities of chief physical interest, namely, the pressure along CA , from which the drag may be obtained by integration, and also the coordinates of the point I , defined by \bar{x} and \bar{y} (Fig. 1). Each of these calculations will now be considered in turn.

PRESSURE DISTRIBUTION

If the pressure coefficient is defined, as is customary, by

$$C_p = \frac{p - p_\infty}{\frac{1}{2} \rho v_\infty^2} \quad (5)$$

then from the definitions of ζ and σ there results

$$C_p = (1 + \sigma) [1 - |\zeta|^2] - \sigma .$$

If one puts $t = \sec \phi$ along the wedge face AC , the pressure coefficient may be expressed as a function of the parameter ϕ by use of Eq. (2ab). For convenience let $P(\phi, \beta) = 1 - |\zeta|^2$ on AC . Then

$$P(\phi, \beta) = 1 - \left[\frac{1 - \sin \phi}{\cos \phi} \right]^{\frac{4\beta}{\pi}}$$

so that

$$C_p = (1 + \sigma) P(\phi, \beta) - \sigma . \quad (6)$$

The total pressure on an element due to both the pressure p on the front and the suction p_k on the back is given by

$$\frac{p - p_k}{\frac{1}{2} \rho v_\infty^2} = (1 + \sigma) P(\phi, \beta) . \quad (7)$$

In order to find the point to which the pressure p corresponds, it is necessary to integrate dy along AC . Now from the relations above,

$$dy = \frac{dy}{dz} \cdot \frac{dz}{dW} \cdot \frac{dW}{dt} dt ,$$

or when the derivatives are evaluated, one has

$$dy = \left(-e^{i\beta} \sin\beta \right) \left(\frac{1}{|\xi|} e^{-i\beta} \right) \left(\frac{b \tan^2 \alpha}{(\tan^2 \alpha + t^2)^{3/2}} \right) dt . \quad (8)$$

However, along AC one may use the substitution $t = \sec \phi$. Also, in what follows it is convenient to consider instead of dy the dimensionless variable dY defined by

$$dY = -(b \sin\beta \sin^2 \alpha \cos \alpha)^{-1} dy . \quad (9)$$

Then in terms of ϕ one has

$$dY = Q(\phi, \beta) \Delta(\phi, \alpha) d\phi \quad (10)$$

where

$$Q(\phi, \beta) = \cos \phi \sin \phi \left[\frac{1 + \sin \phi}{\cos \phi} \right]^{\frac{2\beta}{\pi}} \quad (11)$$

and

$$\Delta(\phi, \alpha) = (1 - \sin^2 \alpha \sin^2 \phi)^{-3/2} . \quad (12)$$

Then, if

$$Y(\phi', \alpha, \beta) = \int_{\phi'}^{\pi/2} dY(\phi, \alpha, \beta) \quad (13)$$

the ordinate of the point in question is located by

$$\frac{y}{a \sin \beta} = \frac{Y(\phi', \alpha, \beta)}{Y(0, \alpha, \beta)} . \quad (14)$$

Therefore by picking values of ϕ' and then computing C_p and $y/a \sin \beta$ from Eqs. (6) and (14), a plot of pressure distribution may be constructed. An example for $\sigma = 0$ is shown in Fig. 3.

While $Y(\phi', \alpha, \beta)$ cannot be integrated in the general case, several special cases can be evaluated. For $\beta = \pi/2$, Plesset and Shaffer give

$$Y(\phi', \alpha, \pi/2) = \sec^2 \alpha \left[\frac{\cos \phi' (1 + \sin \phi')}{(1 - \sin^2 \alpha \sin^2 \phi')^{1/2}} + B(\alpha) - F(\alpha, \phi') + D(\alpha, \phi') \right] \quad (15)$$

where $B(\alpha)$, $F(\alpha, \phi')$, and $D(\alpha, \phi')$ are elliptic integrals in the notation of Ref. 8. For $\phi' = 0$, this reduces to

$$Y(0, \alpha, \pi/2) = \frac{1}{\cos^2 \alpha \sin^2 \alpha} \left[\sin^2 \alpha + E - \cos^2 \alpha K \right] . \quad (16)$$

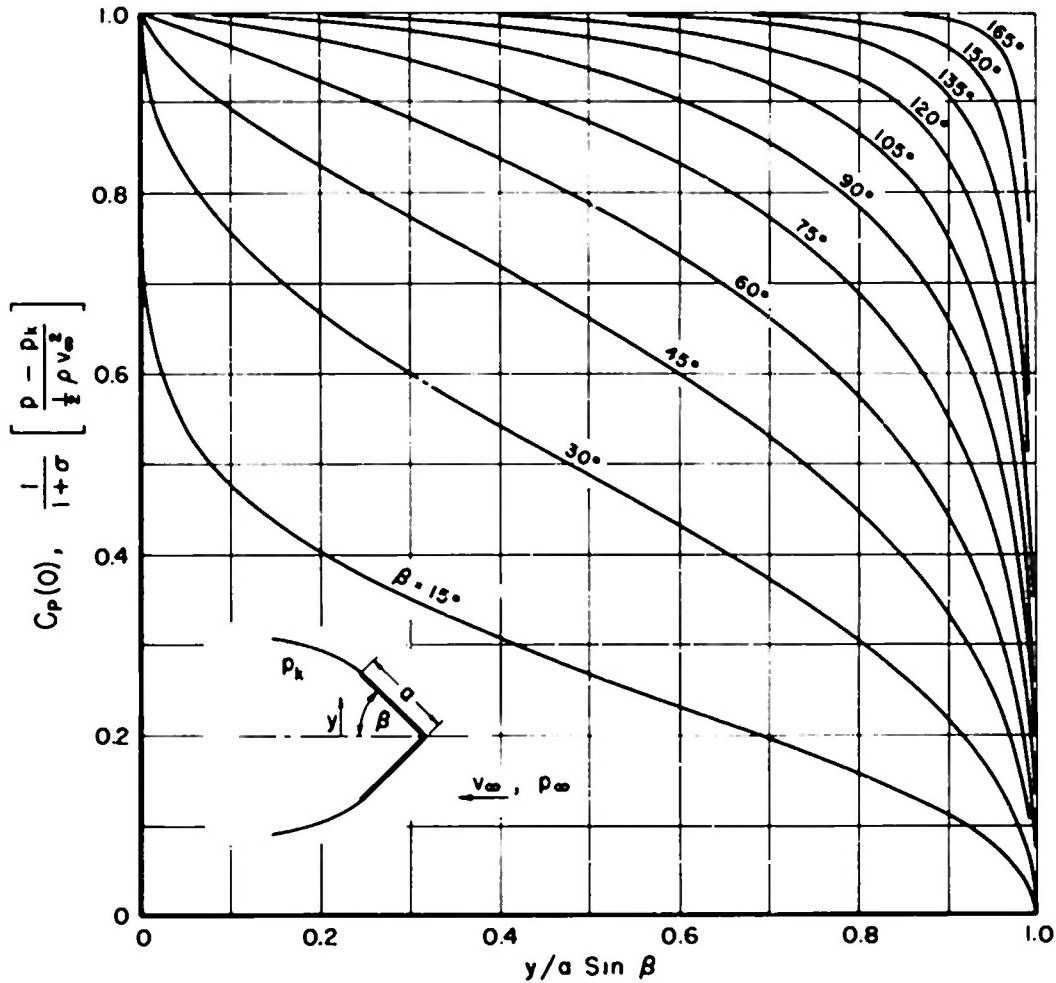


Fig. 3. The pressure distribution on a cavitating wedge (after Plesset and Shaffer). The plot may also be used for any low cavitation number σ by considering the ordinate to be a normalized pressure coefficient as indicated.

Also, one has

$$Y(\phi', 0, \pi/2) = \cos \phi' + \frac{1}{2} \left[\pi/2 - \phi' + \sin \phi' \cos \phi' \right]. \quad (17)$$

If one considers the case $a = 0$, $\beta \neq \pi/2$, corresponding to Bobyleff's problem, the integrals are expressible in general in terms of the logarithmic derivative of the gamma function,⁹

$$Y(0, 0, \beta) = \frac{1}{2} + \frac{\beta}{\pi} + \frac{\beta^2}{2\pi} \left[\Psi \left(1 - \frac{\beta}{2\pi} \right) - \Psi \left(\frac{1}{2} - \frac{\beta}{2\pi} \right) \right] \quad (18)$$

where

$$\Psi(z) = \frac{d}{dz} \log \Gamma(z).$$

If $2\beta/\pi$ is a proper fraction $2\beta/\pi = p/q$, say, where p and q are integers, the integrations may be performed in terms of elementary functions by the substitution $t = (1 - \sin\phi)/(1 + \sin\phi)$ and $t = z^q$. Then in terms of z , the integral is a rational function which may be integrated by standard procedures.

For $\alpha > 0$, the binomial expansion

$$\Delta = 1 + \frac{3}{2} \sin^2 \alpha \sin^2 \phi + \frac{3 \cdot 5}{2 \cdot 4} \sin^4 \alpha \sin^4 \phi + \dots \quad (19)$$

may be employed to obtain

$$Y(0, \alpha, \beta) = Y(0, 0, \beta) + \frac{3}{2} \sin^2 \alpha \int_0^{\frac{\pi}{2}} \sin^2 \phi Q(\phi, \beta) d\phi + \dots \quad (20)$$

where each integral in the series is now integrable by the same procedure as used for $Y(0, 0, \beta)$. In actual practice, it appears that the original tabulations of Plesset and Shaffer, the accuracy of which can readily be checked by comparison with these special cases, will prove adequate for most likely applications. Their results are shown in Table 2, where values for $\alpha = 1^\circ - 4^\circ$ have been added by using the first two terms in Eq. (20) as an interpolation formula.

DRAG IN TWO DIMENSIONS

If the drag coefficient C_D due to a drag force D is defined as

$$C_D = \frac{D}{\frac{1}{2} \rho v_\infty^2 d} \quad (21)$$

where d is the width of the wedge base (Fig. 1), one finds by integration of the total pressure on each element, as given by Eq. (7), that

$$C_D = (\sigma + 1) \frac{\int_0^{\frac{\pi}{2}} P(\phi, \beta) dY(\phi, \alpha, \beta)}{Y(0, \alpha, \beta)} \quad (22)$$

The remarks on the evaluation of $Y(0, \alpha, \beta)$ above also apply to the integral in the numerator. In general, one can employ the expansion Eq. (19) to obtain a series of known integrals. For the special case corresponding to Bobyleff's problem the integration may be performed exactly to obtain

$$\int_0^{\frac{\pi}{2}} P(\phi, \beta) dY(\phi, 0, \beta) = \frac{2}{\pi} \frac{\beta^2}{\sin \beta} \quad (23)$$

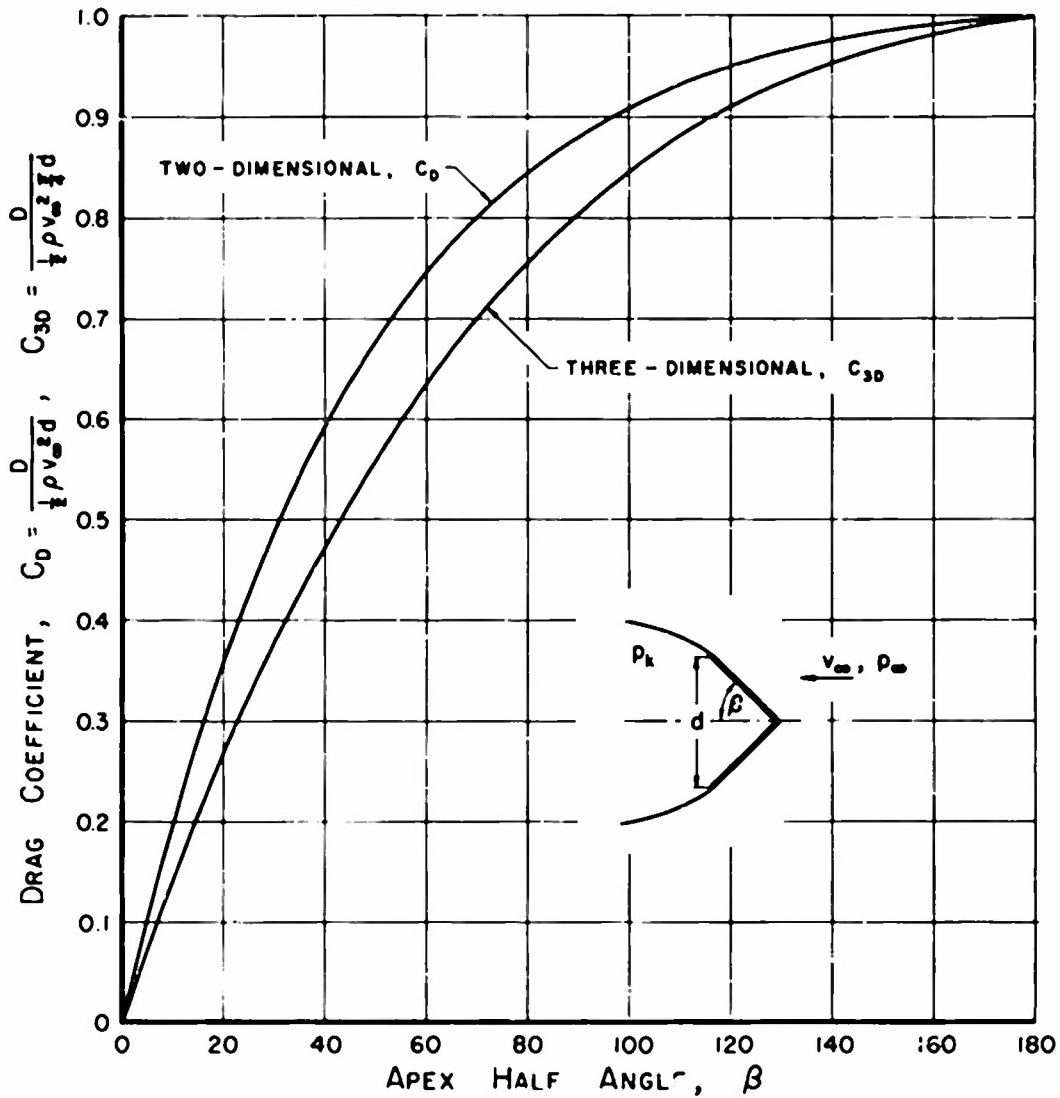


Fig. 4. The two- and three-dimensional drag coefficients at $\sigma = 0$ as a function of β .

and for Riabouchinsky's case

$$\int_0^{\frac{\pi}{2}} P(\phi, \pi/2) dY(\phi, \alpha, \pi/2) = \frac{2}{\cos^2 \alpha \sin^2 \alpha} [E - \cos^2 \alpha K] \quad (24)$$

where E and K are complete elliptic integrals. Hence for these cases the drag coefficients are

$$C_D(0, \beta) = \frac{2}{\pi} \cdot \frac{\beta^2}{\sin \beta Y(0, 0, \beta)} \quad (25)$$

where $Y(0, 0, \beta)$ is given by Eq. (20) and*

$$C_D(\alpha, \pi/2) = 2(\sigma + 1) \left[E(\alpha) - \cos^2 \alpha K(\alpha) \right] . \quad (26)$$

As before, the tabulations of Plesset and Shaffer are in agreement with these formulas, and are presented here for convenience in Table 3 (see also Fig. 4).

DRAG IN THREE DIMENSIONS

The preceding theory is not applicable to the three-dimensional case of an axially symmetrical flow, but Plesset and Shaffer, in view of the lack of any three-dimensional results, proposed to estimate the drag for cones by assuming the distribution of pressure from center to edge was the same as for two dimensions. It is now certain that this is a reasonable estimate, useful enough for many purposes, although a check of the assumption by experiment or other calculations would be of interest.

In any event, when the pressure is integrated on the cone, one obtains for the drag coefficient in three dimensions

$$C_{3D} = 2(\sigma + 1) \frac{\int_{\phi=0}^{\phi=\frac{\pi}{2}} P(\phi, \beta) Y(\phi, \alpha, \beta) d Y(\phi, \alpha, \beta)}{[Y(0, \alpha, \beta)]^2} . \quad (27)$$

The integral in the numerator has been calculated by Plesset and Shaffer for the case $\beta = \pi/2$. Using Eq. (15) for $Y(\phi, \alpha, \pi/2)$, they obtain

$$\int_0^{\frac{\pi}{2}} P Y d Y = \sec^4 \alpha \left[\frac{1}{\sin^2 \alpha} - \frac{n(1+\sigma)}{2 \sin \alpha \tan^2 \alpha} + B^2(\alpha) \right] . \quad (28)$$

In the event $\sigma = \alpha = 0$, the integrations may be performed directly or the limit of the above expression taken to find

$$\int_0^{\frac{\pi}{2}} P(\phi, \beta) Y(\phi, 0, \pi/2) d Y(\phi, 0, \pi/2) = \frac{2}{3} + \frac{\pi^2}{16} . \quad (29)$$

so the zero-cavitation number drag of a disk is

* The formula for C_D given by Plesset and Shaffer, Eq. (25), Ref. 4, and Eq. (25), Ref. 5, is incorrect by a factor of 2.

$$C_{3D}(0, \pi/2) = \frac{2/3 + \pi^2/16}{1 + \pi/4} = 0.8053 \quad (30)$$

The tabulations of Plesset and Shaffer for the drag coefficient are given in Table 4 and are believed accurate enough for any engineering purpose (see also Fig. 4).

CAVITY SHAPE IN TWO DIMENSIONS

The location of the maximum width of the cavity (Fig. 1) is given by

$$\bar{y} = \int_{AI} \sin \theta |dz| \quad \text{and} \quad \bar{x} = \int_{AI} \cos \theta |dz| \quad (31)$$

where $\theta = \arg \zeta$ is the slope of the cavity wall and the integration is to be performed along the free streamline from A to I. Now if $\arg \eta = \psi = \pi \theta / 2\beta$ along AIA' one has

$$t = \sin \psi = \sin (\pi \theta / 2\beta) .$$

Also, on this contour, since $|\zeta| = 1$, then $|dz| = |dW|$ from Eq. (3) and hence, from Eq. (2c) and the above value for t ,

$$|dz| = (\cos a \sin^3 a) b \Delta' \cos \psi d\psi$$

where

$$\Delta' = (1 - \cos^2 a \cos^2 \psi)^{-3/2} .$$

Then, by employing Eq. (9) to obtain dimensionless forms, one finds that

$$\frac{\bar{x}}{a} = \frac{R(a, \beta)}{Y(0, a, \beta)} \quad (32)$$

and

$$\frac{\bar{y}}{a} = \frac{S(a, \beta)}{Y(0, a, \beta)} \quad (33)$$

where for convenience the abbreviations

$$R(a, \beta) = \int_0^{\pi/2} \cos \left(\frac{2\beta}{\pi} \psi \right) \cos \psi \Delta' d\psi \quad , \quad (34)$$

and

$$S(\alpha, \beta) = \int_0^{\frac{\pi}{2}} \sin\left(\frac{2\beta}{\pi} \psi\right) \sin \psi \Delta' d\psi \quad (35)$$

have been used. (If one wished to plot the shape of the cavity wall, the lower limits would be changed accordingly.)

The integrals $R(\alpha, \beta)$ and $S(\alpha, \beta)$ have been computed by expanding $\sin(2\beta\psi/\pi)$ and $\cos(2\beta\psi/\pi)$ in Fourier series, and then integrating term by term. Hence the construction of suitable series for $\sin \lambda\psi$ and $\cos \lambda\psi$ will now be considered, where $\lambda = 2\beta/\pi$.

EXPANSION IN SERIES OF $\sin \lambda\psi$ AND $\cos \lambda\psi$

if λ is not an integer, the well-known series¹⁰

$$\cos \lambda\psi = \frac{2\lambda}{\pi} \sin \lambda\pi \left[\frac{1}{2\lambda^2} + \sum_{n=1}^{\infty} (-1)^{n+1} \frac{\cos n\psi}{n^2 - \lambda^2} \right]$$

is convergent and may be integrated term by term. When this is done three times (the constants of integration being properly evaluated), the following series is obtained:

$$\sin \lambda\psi = G_\lambda \psi + H_\lambda \psi^3 + \sum_{n=1}^{\infty} D_{n,\lambda} \sin n\psi \quad (36)$$

where for convenience the notation has been used that

$$G_\lambda = \lambda - \lambda^4 \left(\frac{2}{\pi} \sin \lambda\pi \right) \sum_{n=1}^{\infty} (-1)^{n+1} \frac{1}{n^2(n^2 - \lambda^2)} \quad (36a)$$

$$H_\lambda = -\frac{\lambda^2}{\pi} \cdot \frac{2}{\pi} \sin \lambda\pi \quad (36b)$$

and

$$D_{n\lambda} = \lambda^4 \left(\frac{2}{\pi} \sin \lambda\pi \right) \frac{(-1)^{n+1}}{n^3(n^2 - \lambda^2)} \quad (36c)$$

It is now necessary to find trigonometric series for ψ and ψ^3 . These can easily be constructed from the series¹⁰

$$\psi^2 = \frac{\pi^2}{4} - \frac{8}{\pi} \sum_{n=1}^{\infty} (-1)^{n+1} \frac{\cos(2n+1)\psi}{(2n+1)^3} \quad (37)$$

and

$$\psi^3 - \pi^2 \psi = -12 \sum_{n=1}^{\infty} (-1)^{n+1} \frac{\sin n \psi}{n^3} \quad (38)$$

since integration of the first yields an expression for $\psi^3 - 3\pi^2/4$, which can then be solved simultaneously with the second to obtain two new series, one for ψ , and one for ψ^3 . These are

$$\psi = \sum_{n=1}^{\infty} B_n \sin n \psi \quad (39)$$

and

$$\psi^3 = \sum_{n=1}^{\infty} F_n \sin n \psi \quad (40)$$

where

$$B_n = \frac{11,520}{7\pi^4} \cdot \frac{1}{n^5} \left[1 - (-1)^{\frac{n+1}{2}} \frac{2}{n\pi} + \frac{n\pi}{12} \right], \quad n=1, 3, 5, \dots, \quad (41)$$

$$B_n = -\frac{11,520}{7\pi^4} \cdot \frac{1}{n^5}, \quad n=2, 4, 6, \dots,$$

and

$$F_n = \frac{24 \times 360}{7\pi^2} \cdot \frac{1}{n^5} \left[1 - (-1)^{\frac{n+1}{2}} \frac{2}{n\pi} + n \frac{37\pi}{360} \right], \quad n=1, 3, 5, \dots, \quad (42)$$

$$F_n = -\frac{24 \times 360}{7\pi^2} \cdot \frac{1}{n^5}, \quad n=2, 4, 6, \dots$$

Then the series for $\sin \lambda \psi$ can now be written

$$\sin \lambda \psi = \sum_{n=1}^{\infty} g_n \sin n \psi \quad (43)$$

where

$$g_n = G_\lambda B_n + H_\lambda F_n + D_{n\lambda}. \quad (43a)$$

Also the above series for $\sin \lambda \psi$ may be integrated once to obtain

$$\cos \lambda \psi = h_0 + \lambda \sum_{n=1}^{\infty} h_n \cos n \psi \quad (44)$$

in which

$$h_0 = 1 - \lambda \sum_{n=1}^{\infty} \frac{g_n}{n} \quad (44a)$$

and

$$h_n = g_n/n \quad (44b)$$

The values for g_n and h_n are presented in Table 10.

EVALUATION OF INTEGRALS $R(\alpha, \beta)$ AND $S(\alpha, \beta)$

The problem of finding the integrals $R(\alpha, \beta)$ and $S(\alpha, \beta)$ can now, by applying Eqs. (43) and (44), be reduced to summing infinite series which contain integrals of the type

$$I_n = \int_0^{\frac{\pi}{2}} \sin n \psi \Delta'(\psi) d\psi \quad (45)$$

and

$$J_n = \int_0^{\frac{\pi}{2}} \cos n \psi \Delta'(\psi) d\psi \quad (46)$$

By writing $\sin n \psi$ and $\cos n \psi$ in terms of powers and products of $\sin \psi$ and $\cos \psi$, the integrals I_n and J_n can be written as sums of integrals of the type

$$\int_0^{\frac{\pi}{2}} \sin^p \psi \cos^q \psi \Delta'(\psi) d\psi \quad (47)$$

Such integrals can always be reduced by integration by parts to known elementary functions or complete elliptic integrals. For the present work, values of the integrals I_n and J_n have been computed for a range of α , and the results are shown in Table 9. Also an estimate of ΔI is shown, where

$$\Delta I = I_{n+1} - I_n, \quad n > 6 \quad (48)$$

since this quantity is used in a later computation.

With the values of A_n , b_n , I_n , and J_n , it is easy to find R and S , since, from above, there results

$$R(\alpha, \beta) = \frac{h_0}{\sin^2 \alpha} + \lambda \sum_{n=1}^{\infty} h_n J_n \quad (49)$$

and

$$S(\alpha, \beta) = \sum_{n=1}^{\infty} g_n I_n \quad (50)$$

These series were computed for a sufficient number of terms to assure reasonable accuracy. In the case of $R(\alpha, \beta)$, the series converges very rapidly so that only five terms are necessary to obtain an accuracy of $\pm 0.1\%$. The series for $S(\alpha, \beta)$, however, requires at least seven terms, and a further correction was made by a procedure as follows.

If α is small, the values of $(I_{n+1} - I_n)$ are almost equal for $n > 6$ or so, as can be seen from Table 9. Hence for an improved estimate of S we write

$$S(\alpha, \beta) = \sum_{n=1}^7 g_n I_n + I_8 \sum_{n=8}^{13} g_n + (\Delta I) \sum_{n=8}^{13} (n-8) g_n \quad (51)$$

For $\alpha \geq 5^\circ$, the resulting values are accurate to within $\pm 0.1\%$, while for $\alpha < 5^\circ$, the values obtained are within $\pm 0.15\%$. A summary of these results is given in Tables 5 and 6. The values of $R(\alpha, \beta)$ and $S(\alpha, \beta)$ have then been used with those for $Y(0, \alpha, \beta)$ from Table 2, to find \bar{x}/a and \bar{y}/a ; the results are presented in Tables 7 and 8.

For the case of $\beta = \pi/2$, the integral $R(\alpha, \beta)$ can be expressed in terms of elliptic integrals and $S(\alpha, \beta)$ can be expressed by simple functions, as was shown by Riabouchinsky. There results

$$R(\alpha, \frac{\pi}{2}) = \frac{1}{\sin^2 \alpha \cos^2 \alpha} \left[E'(\alpha) - \sin^2 \alpha K'(\alpha) \right] \quad (52)$$

and

$$S(\alpha, \frac{\pi}{2}) = \frac{1 - \sin \alpha}{\cos^2 \alpha \sin \alpha} \quad (53)$$

Then for Riabouchinsky's case

$$\frac{\bar{x}}{a} = \frac{E' - \sin^2 \alpha K}{\sin^2 \alpha + E - \cos^2 \alpha K} \quad (54)$$

and

$$\frac{\bar{y}}{a} = \sin \alpha \frac{1 - \sin \alpha}{\sin^2 \alpha + E - \cos^2 \alpha K} \quad (55)$$

The values from these equations are included in Tables 5, 6, 7 and 8.

The principal cavity dimensions can now be calculated from the formulas

$$\frac{d_m}{d} = 1 + \csc \beta \frac{\bar{y}}{a} \quad (56)$$

and

$$\frac{g}{d} = \cot \beta + \csc \beta \frac{\bar{x}}{a} \quad (57)$$

These parameters are plotted in Figs. 5 and 6. In Fig. 7, the ratio g/d_m is shown. This will be discussed further in the section below concerning asymptotic values.

APPROXIMATIONS FOR LOW CAVITATION NUMBERS

If the cavitation number σ is small, which implies that α is small, suitable approximation may be made to evaluate the several integrals discussed above. For example, in calculating the drag coefficients, one may use the first approximations

$$Y(0, \alpha, \beta) = Y(0, 0, \beta) + O(\alpha^2); \quad (58)$$

and

$$\int_0^{\frac{\pi}{2}} P d Y(0, \alpha, \beta) = \int_0^{\frac{\pi}{2}} P d Y(0, 0, \beta) + O(\alpha^2) \quad (59)$$

so that the drag coefficient becomes, as is well known,

$$C_D = (1 + \sigma) C_D(0, \beta) + O(\alpha^2) \quad (60)$$

The same approximation holds for three dimensions.

For computing the pressure distribution one may then use the approximation for small α

$$\frac{Y(\phi, \alpha, \beta)}{Y(0, \alpha, \beta)} \approx \frac{Y(\phi, 0, \beta)}{Y(0, 0, \beta)} \quad (61)$$

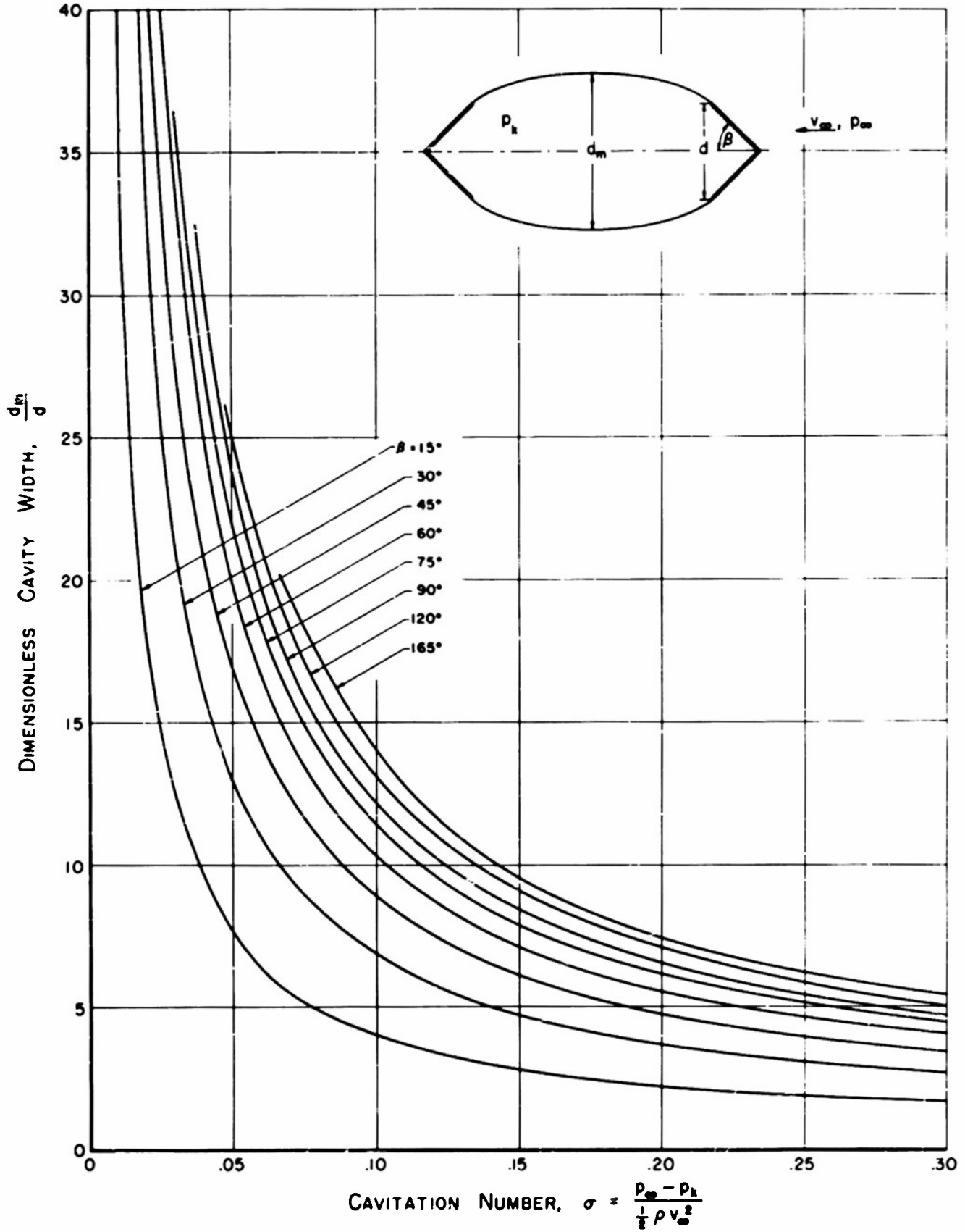


Fig. 5. The width of a two-dimensional cavity.

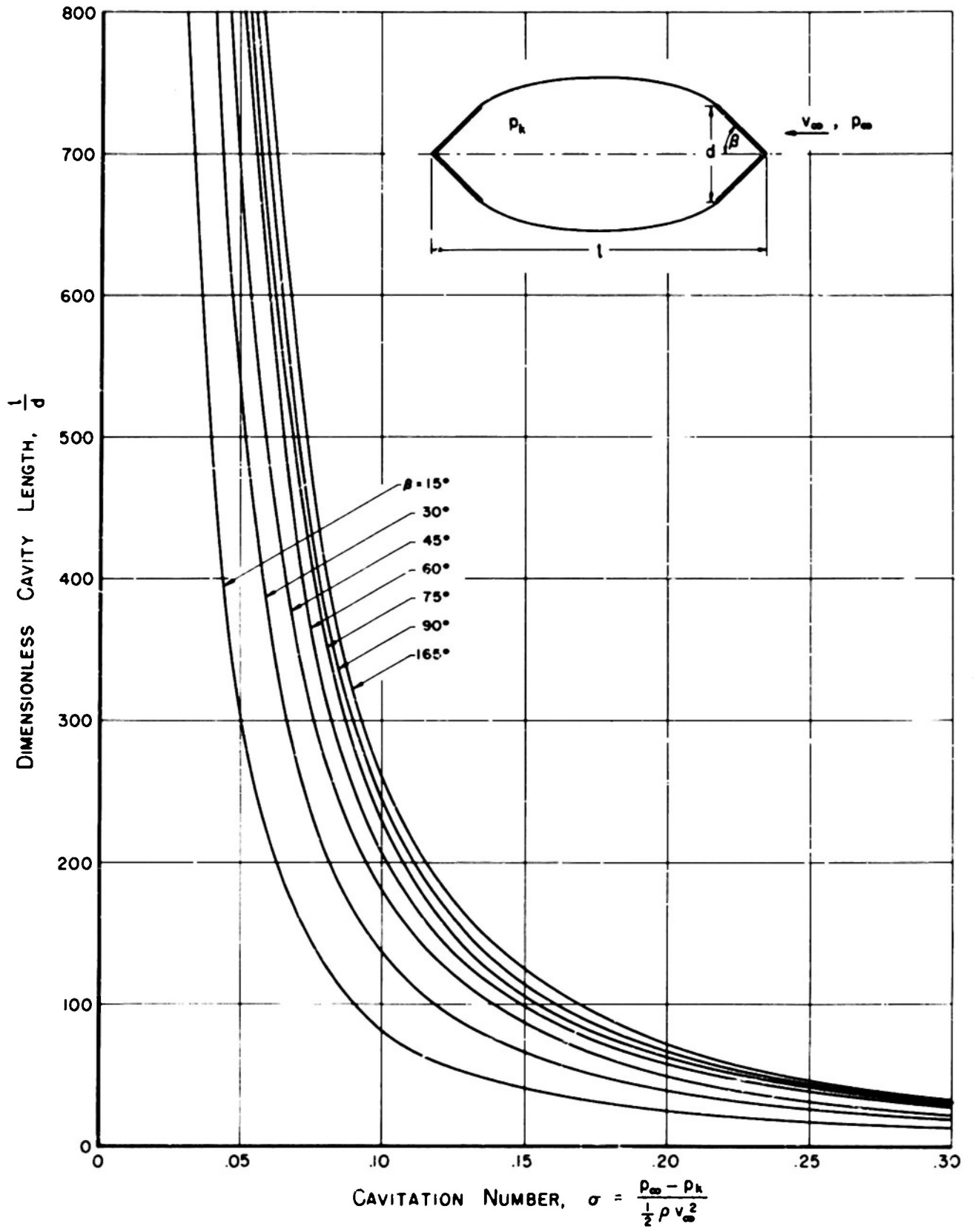


Fig. 6. The length of a two-dimensional cavity.

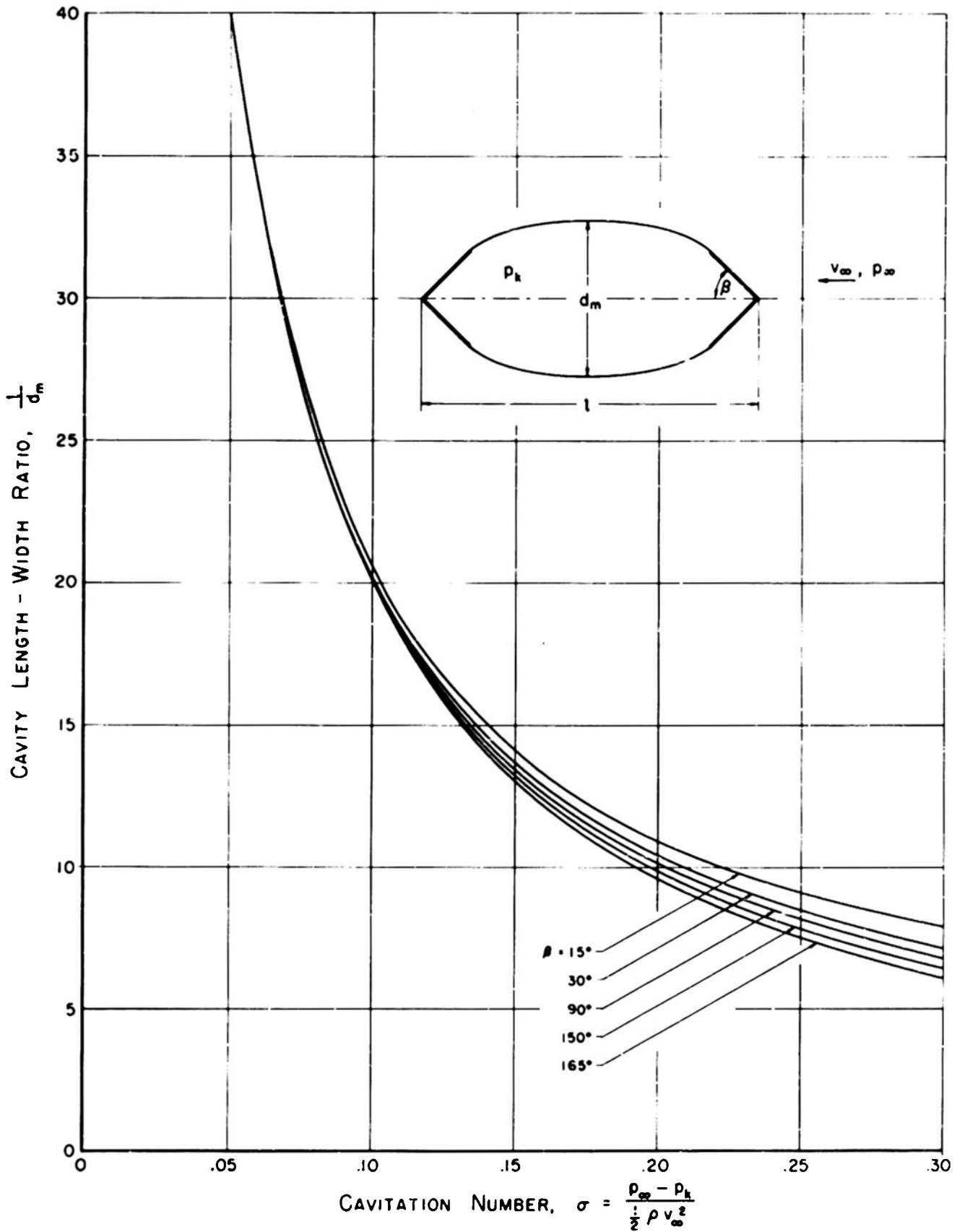


Fig. 7. The length-width ratio of a two-dimensional cavity. At very low σ , the ratio is independent of β , being asymptotic to $2/\sigma$.

If instead of the pressure one plots

$$\frac{1}{1+\sigma} \frac{P - P_k}{\frac{1}{2} \rho v_{\infty}^2} = P(\phi, \beta) \quad (62)$$

a dimensionless representation is obtained which is exact when $\alpha = 0$ and is a useable approximation for any small cavitation number (Fig. 3). The accuracy of the approximation may be noted by comparison with the exact values in Ref. 5. It appears that the error will be less than a percent or so if $\alpha \leq 5^\circ$ (see Table 1 for corresponding values of σ).

To find $R(\alpha, \beta)$ and $S(\alpha, \beta)$ when the cavitation number is small, it is only necessary to obtain approximations for $\sin \lambda \psi$ and $\cos \lambda \psi$ which are accurate near the origin. For this purpose one may write $\sin \lambda \psi \approx \lambda \sin \psi$. Then

$$\cos \lambda \psi \approx 1 - \frac{\lambda^2}{2} \sin^2 \psi, \quad (63)$$

so that for a first approximation

$$\begin{aligned} R &= \int_0^{\frac{\pi}{2}} \left(1 - \frac{\lambda^2}{2} \sin^2 \psi\right) \cos \psi \Delta'(\psi, \alpha) d\psi \\ &= \int_0^{\frac{\pi}{2}} \cos \psi \Delta'(\psi, \alpha) d\psi - \frac{\lambda^2}{2} \int_0^{\frac{\pi}{2}} \sin^2 \psi \cos \psi \Delta'(\psi, \alpha) d\psi \\ &= \frac{1}{\sin^2 \alpha} - \frac{\lambda^2}{2} \frac{1}{\cos^2 \alpha} - 1 + \frac{1}{2 \cos \alpha} \ln \frac{1 + \cos \alpha}{1 - \cos \alpha}. \end{aligned} \quad (64)$$

For $\alpha \rightarrow 0$, we have

$$R(\alpha, \beta) = \frac{1}{\sin^2 \alpha}. \quad (65)$$

As $\alpha \rightarrow 0$, the approximation $\sin \lambda \psi = \lambda \sin \psi$ may also be used to evaluate S , so

$$\begin{aligned} S(\alpha, \beta) &= \lambda \int_0^{\frac{\pi}{2}} \sin \psi \cos \psi \Delta' d\psi \\ &= \frac{\lambda}{\sin \alpha}. \end{aligned} \quad (66)$$

Then for $\alpha \rightarrow 0$ the cavity length-width ratio becomes

$$\frac{l}{d_m} = \frac{R(\alpha, \beta)}{S(\alpha, \beta)} = \frac{1}{\lambda \sin \alpha} \quad (67)$$

But for $\alpha \rightarrow 0$ we have

$$\sigma = 2\lambda \sin \alpha \quad (68)$$

so that

$$\frac{l}{d_m} = \frac{2}{\sigma} \quad (69)$$

Hence at low cavitation numbers the principal cavity dimensions are independent of nose shape, being functions of σ only. A similar result was found by Reichardt¹¹ for three-dimensional cavities.

It will be found that the approximations given above will enable extension of the values in Tables 5, 6, 7, and 8 to lower cavitation numbers with reasonable accuracy.

REFERENCES

1. Durand, W. F., (editor), Aerodynamic Theory, Vol. II, Julius Springer, Berlin, 1935.
2. Riabouchinsky, D., Proc. Lond. Math. Soc. (Ser. 2), Vol. 19, pp. 206-215, 1920.
3. Plesset, M. S., and Shaffer, P. A., Jr., "Drag in Cavitating Flow", Reviews of Modern Physics, Vol. 20, No. 1, pp. 228-231, January, 1948.
4. Plesset, M. S., and Shaffer, P. A., Jr., "Cavity Drag in Two and Three Dimensions", Journal of Applied Physics, Vol. 19, No. 10, pp. 934-939, October, 1948.
5. Plesset, M. S., and Shaffer, P. A., Jr., "Cavity Drag in Two and Three Dimensions", U. S. Naval Ordnance Test Station, Navord Report No. 1014, Pasadena, October, 1949.
6. Lamb, H., Hydrodynamics, 6th ed., pp. 104-105, Cambridge University Press, 1932.
7. Fisher, J. W., "Discontinuous Flow with Cavity Formation", H.M. A/S. E.E. Internal Report No. 217, April, 1945.
8. Jahnke, E., and Emde, F., Tables of Functions, Dover Publications, New York, 1945.
9. Milne-Thompson, L. M., Theoretical Hydrodynamics, 2nd ed., The Macmillan Company, New York, 1950.
10. Dwight, H. B., Tables of Integrals and Other Mathematical Data, revised ed., The Macmillan Company, New York, 1947.
11. Reichardt, H., "The Laws of Cavitation Bubbles at Axially Symmetrical Bodies in a Flow", Reports and Translations No. 766, Ministry of Aircraft Production, 1946 (distributed by Office of Naval Research, Navy Dept., Washington, D.C.).

TABLE 1 - THE CAVITATION NUMBER, $\sigma(a, \beta)$

a	$\beta=15^\circ$	30°	45°	60°	75°	90°	105°	120°	135°	150°	165°
0°	0.0000	0.0000	0.0000	0.0000	0.0000	0.0000	0.0000	0.0000	0.0000	0.0000	0.0000
1	0.0058	0.0117	0.0176	0.0235	0.0295	0.0355	0.0416	0.0476	0.0538	0.0599	0.0661
2	0.0117	0.0235	0.0355	0.0476	0.0598	0.0722	0.0848	0.0974	0.1103	0.1232	0.1364
3	0.0176	0.0356	0.0538	0.0724	0.0913	0.1105	0.1301	0.1500	0.1702	0.1909	0.2118
4	0.0236	0.0477	0.0724	0.0977	0.1235	0.1500	0.1771	0.2049	0.2333	0.2623	0.2921
5	0.0296	0.0600	0.0913	0.1236	0.1568	0.1910	0.2262	0.2624	0.2997	0.3381	0.3777
10	0.0602	0.1241	0.1918	0.2635	0.3396	0.4203	0.5058	0.5965	0.6925	0.7945	0.9026
15	0.0923	0.1931	0.3032	0.4235	0.5549	0.6984	0.8551	1.0264	1.2134	1.4177	1.6408
20	0.1261	0.2682	0.4281	0.6083	0.8112	1.0396	1.2969	1.5866	1.9129	2.2803	2.6940
25	0.1622	0.3506	0.5697	0.8242	1.1201	1.4639	1.8635	2.3279	2.8676	3.4948	4.2237
30	0.2009	0.4423	0.7321	1.0801	1.4981	2.0000	2.6028	3.3267	5.1962		
35	0.2431	0.5453	0.9210	1.3880	1.9685	2.6902	3.5873				
40	0.2896	0.6630	1.1445	1.7655	2.5663	3.5989					
45	0.3415	0.7996	1.4142	2.2387	3.3447						

TABLE 2 - THE INTEGRAL $Y(0, a, \beta)$

a	$\beta=15^\circ$	30°	45°	60°	75°	90°	105°	120°	135°	150°	165°
0°	0.59401	0.71443	0.87184	1.08229	1.37195	1.78543	2.40471	3.39686	5.15664	8.87842	20.55725
1	0.59415	0.71461	0.87208	1.08260	1.37237	1.78601	2.40555	3.39809	5.15863	8.88205	20.56616
2	0.59458	0.71517	0.87278	1.08353	1.37362	1.78774	2.40801	3.40180	5.16459	8.89293	20.59291
3	0.59531	0.71609	0.87396	1.08509	1.37571	1.79062	2.41213	3.40797	5.17452	8.91108	20.63746
4	0.59631	0.71738	0.87562	1.08727	1.37864	1.79466	2.41791	3.41660	5.18844	8.93647	20.69935
5	0.59760	0.71904	0.87774	1.09007	1.38240	1.79985	2.42533	3.42771	5.20632	8.96913	20.78006
10	0.60858	0.73300	0.89582	1.11385	1.41436	1.84399	2.48844	3.52238	5.35898	9.24832	21.46678
15	0.62762	0.75736	0.92745	1.15575	1.47115	1.92315	2.60292	3.69665	5.64503	9.78311	22.81780
20	0.65529	0.79276	0.97331	1.21622	1.55255	2.03556	2.76341	3.93657	6.02969	10.48055	24.51212
25	0.69356	0.84189	1.03744	1.30136	1.66807	2.19659	2.99594	4.28896	6.60392	11.54241	27.15383
30	0.74451	0.90768	1.12366	1.41646	1.82512	2.41681	3.31584	4.77666	7.40369	13.03090	30.88178
35	0.81149	0.99468	1.23846	1.57076	2.03710	2.71615	3.75382	5.44951	8.51562	15.11691	36.14913
40	0.89944	1.10981	1.35153	1.77819	2.32453	3.12554	4.35817	6.38651	10.07890	18.07856	43.70293
45	1.01573	1.26347	1.59791	2.06056	2.71977	3.69456	5.20743	7.71805	12.32599	22.38586	54.82158

TABLE 3 - DRAG COEFFICIENTS FOR TWO-DIMENSIONAL WEDGES, $C_D(a, \beta)$

a	$\beta=15^\circ$	30°	45°	60°	75°	90°	105°	120°	135°	150°	165°
0°	0.2838	0.4885	0.6370	0.7448	0.8230	0.8798	0.9207	0.9498	0.9703	0.9845	0.9939
5	0.2927	0.5185	0.6959	0.8375	0.9528	1.0482	1.1293	1.1993	1.2613	1.3176	1.3694
10	0.3029	0.5521	0.7624	0.9443	1.1057	1.2522	1.3885	1.5180	1.6436	1.7674	1.8914
15	0.3146	0.5901	0.8385	1.0688	1.2880	1.5016	1.7142	1.9297	2.1514	2.3825	2.6259
20	0.3281	0.6330	0.9258	1.2148	1.5073	1.8097	2.1279	2.4676	2.8346	3.2346	3.6741
25	0.3436	0.6826	1.0278	1.3859	1.7754	2.1966	2.6621	3.1825	3.7695	4.4364	5.1975
30	0.3618	0.7401	1.1481	1.5993	2.1080	2.6898	3.3634	4.1497	5.0738		
35	0.3829	0.8076	1.2922	1.8574	2.5274	3.3308	4.3031				
40	0.4080	0.8880	1.4676	2.1803	3.0676	4.1830					
45	0.4378	0.9853	1.6852	2.5927	3.7806						

TABLE 4 - DRAG COEFFICIENTS FOR CONES OF REVOLUTION, $C_D(a, \beta)$

a	$\beta=15^\circ$	30°	45°	60°	75°	90°	105°	120°	135°	150°	165°
0°	0.2045	0.3758	0.5181	0.6350	0.7296	0.8053	0.8646	0.9101	0.9442	0.9693	0.9874
5	0.2108	0.3990	0.5664	0.7143	0.8450	0.9599	1.0609	1.1495	1.2276	1.2972	1.3604
10	0.2184	0.4255	0.6213	0.8064	0.9817	1.1477	1.3054	1.4559	1.6004	1.7407	1.8792
15	0.2275	0.4557	0.6849	0.9147	1.1459	1.3787	1.6140	1.8527	2.0966	2.3478	2.6097
20	0.2379	0.4906	0.7586	1.0429	1.3445	1.6683	2.0072	2.3725	2.7649	3.1891	3.6525
25	0.2501	0.5311	0.8456	1.1969	1.5892	2.0274	2.5171	3.0655	3.6817	4.3779	5.1686
30	0.2648	0.5788	0.9494	1.3847	1.8950	2.4918	3.1898	4.0061	4.9635		
35	0.2818	0.6355	1.0749	1.6173	2.2835	3.0988	4.0950				
40	0.3022	0.7039	1.2296	1.9110	2.7882	3.9209					
45	0.3270	0.7875	1.4236	2.2899	3.4593						

TABLE 5 - THE INTEGRAL $R(\alpha, \beta)$

α	$\beta=15^\circ$	30°	45°	60°	75°	90°	105°	120°	135°	150°	165°
0°	∞	∞	∞	∞	∞	∞	∞	∞	∞	∞	∞
1	3283.1	3283.1	3282.9	3282.6	3282.0	3281.2	3280.5	3279.9	3279.5	3279.1	3278.2
2	821.00	820.89	820.68	820.37	819.98	819.41	818.84	818.22	817.63	816.97	816.14
3	365.06	364.95	364.76	364.51	364.12	363.68	363.17	362.63	362.05	361.42	360.69
4	205.48	205.37	205.20	204.96	204.63	204.23	203.79	203.29	202.76	202.18	201.52
5	131.61	131.52	131.36	131.13	130.83	130.47	130.07	129.61	129.12	128.59	128.00
10	33.139	33.067	32.948	32.781	32.569	32.315	32.021	31.694	31.337	30.955	30.551
15	14.909	14.851	14.755	14.622	14.455	14.256	14.027	13.773	13.498	13.205	12.898
20	8.5323	8.4838	8.4038	8.2936	8.1553	7.9908	7.8037	7.5965	7.3726	7.1352	6.8870
25	5.5853	5.5447	5.4778	5.3854	5.2690	5.1222	4.9723	4.7969	4.6073	4.4068	4.1988
30	3.9877	3.9512	3.8910	3.8086	3.7056	3.5836	3.4460	3.2947	3.1328	2.9631	2.7885

TABLE 6 - THE INTEGRAL $S(\alpha, \beta)$

α	$\beta=15^\circ$	30°	45°	60°	75°	90°	105°	120°	135°	150°	165°
0°	∞	∞	∞	∞	∞	∞	∞	∞	∞	∞	∞
1	9.4323	18.861	28.273	37.659	47.011	56.316	65.578	74.790	83.966	93.175	102.36
2	4.6529	9.3010	13.936	18.550	23.136	27.687	32.204	36.678	41.116	45.546	49.939
3	3.0615	6.1179	9.1618	12.187	15.188	18.157	21.094	23.994	26.857	29.700	32.504
4	2.2668	4.5235	6.7784	9.0108	11.220	13.401	15.551	17.665	19.744	21.797	23.811
5	1.7910	3.5768	5.3514	7.1091	8.8450	10.554	12.234	13.879	15.490	17.073	18.617
10	0.84477	1.6845	2.5155	3.3322	4.1306	4.9067	5.6579	6.3804	7.0725	7.7340	8.3608
15	0.53607	1.0678	1.5909	2.1013	2.5953	3.0693	3.5030	3.9479	4.3480	4.7200	5.0635
20	0.38504	0.76618	1.1396	1.5016	1.8490	2.1787	2.4879	2.7749	3.0384	3.2772	3.4904
25	0.29716	0.59074	0.87732	1.1535	1.4164	1.6633	1.8918	2.1002	2.2874	2.4524	2.5945
30	0.24052	0.47777	0.70856	0.92985	1.1389	1.3333	1.5110	1.6704	1.8106	1.9306	2.0300

TABLE 7 - THE PARAMETER \bar{x}/a WHICH FIXES THE CAVITY LENGTH (Fig. 1)

α	$\beta=15^\circ$	30°	45°	60°	75°	90°	105°	120°	135°	150°	165°
0°	∞	∞	∞	∞	∞	∞	∞	∞	∞	∞	∞
1	5526.	4594.	3764.	3032.	2392.	1837.	1364.	965.2	635.7	369.2	159.4
2	1381.	1148.	940.3	757.1	597.0	458.4	340.0	240.5	158.3	91.87	39.63
3	613.2	509.6	417.4	335.9	264.7	203.1	150.6	106.4	69.97	40.56	17.48
4	344.6	286.3	234.4	186.5	148.4	113.8	84.28	59.50	39.08	22.62	9.736
5	220.2	182.9	149.6	120.3	94.64	72.49	53.63	37.81	24.80	14.34	6.160
10	54.45	45.11	36.78	29.43	23.03	17.52	12.87	8.998	5.848	3.347	1.423
15	23.75	19.61	15.91	12.65	9.826	7.422	5.389	3.726	2.391	1.350	0.565
20	13.02	10.70	8.634	6.819	5.253	3.926	2.824	1.930	1.223	0.681	0.281
25	8.053	6.586	5.280	4.138	3.159	2.332	1.660	1.118	0.698	0.382	0.155
30	5.356	4.353	3.463	2.689	2.030	1.483	1.039	0.690	0.423	0.227	0.093
35	3.732	3.012	2.376	1.826	1.363	0.983	0.679				
40	2.680	2.145	1.676	1.274	0.939	0.668					
45	1.960	1.554	1.201	0.902	0.656	0.459					

TABLE 8 - THE PARAMETER \bar{y}/a WHICH FIXES THE CAVITY WIDTH (Fig. 1)

α	$\beta=15^\circ$	30°	45°	60°	75°	90°	105°	120°	135°	150°	165°
0°	∞	∞	∞	∞	∞	∞	∞	∞	∞	∞	∞
1	15.88	26.39	32.42	34.79	34.26	31.53	27.26	22.01	16.28	10.49	4.977
2	7.826	13.01	15.97	17.12	16.84	15.49	13.37	10.78	7.961	5.122	2.425
3	5.143	8.544	10.48	11.23	11.04	10.14	8.745	7.040	5.190	3.333	1.575
4	3.801	6.313	7.741	8.288	8.138	7.467	6.431	5.170	3.805	2.439	1.150
5	2.997	4.974	6.097	6.522	6.398	5.864	5.044	4.049	2.975	1.904	0.896
10	1.388	2.298	2.808	2.992	2.920	2.661	2.274	1.811	1.320	0.836	0.389
15	0.851	1.410	1.715	1.818	1.764	1.598	1.346	1.068	0.770	0.482	0.222
20	0.588	0.966	1.171	1.235	1.191	1.070	0.900	0.705	0.504	0.313	0.142
25	0.428	0.702	0.846	0.886	0.849	0.757	0.631	0.490	0.346	0.212	0.096
30	0.323	0.526	0.630	0.656	0.624	0.552	0.456	0.350	0.244	0.148	0.066
35	0.248	0.403	0.478	0.494	0.466	0.408	0.333				
40	0.193	0.311	0.366	0.375	0.350	0.303					
45	0.151	0.240	0.280	0.284	0.262	0.224					

TABLE 9 - THE INTEGRALS $I_n(a)$, ΔI , AND $J_n(a)$

a	I_1	I_2	I_3	I_4	I_5	I_6	I_7	ΔI	J_1	J_2	J_3
1°	56.316	111.524	165.084	217.04	267.59	316.80	364.62	46	3281.3	3275.7	3267.5
2	27.687	54.300	79.328	102.84	125.08	146.12	165.95	18	819.42	814.93	808.42
3	18.157	35.270	50.859	65.023	78.020	89.957	100.73	8	363.68	359.77	354.27
4	13.401	25.787	36.707	46.283	54.796	62.367	69.010	5	204.24	200.76	195.97
5	10.554	20.122	28.277	35.166	41.084	46.169	50.442	2	130.477	127.326	123.024
10	4.9067	9.9518	11.798	13.726	14.940	15.900	16.109	-0.4	32.314	30.124	27.346
15	3.0693	5.3772	6.6837	7.2059	7.4500	7.2652	7.1364	-0.3	14.256	12.580	10.576
20	2.1787	3.6775	4.3150	4.3886	4.2591	4.0656	3.7990	-0.3	7.9910	6.6307	5.1142
25	1.6633	2.7136	3.0134	2.8717	2.6356	2.4177	2.1842	-0.2	5.1306	3.9865	2.8047
30	1.3333	2.1088	2.2222	1.9862	1.7284	1.5364	1.3532	-0.2	3.5839	2.6121	1.6396
35	1.1080	1.7037	1.7084	1.4334	1.1868	1.0326	0.8971		2.6561	1.8204	0.8912
40	0.9470	1.4196	1.3588	1.0715	0.8469	0.7289	0.6308		2.0859	1.3322	0.6416
45	0.8284	1.2140	1.1127	0.8260	0.6255	0.5381	0.4683		1.6942	1.0140	0.4150

TABLE 10 - THE COEFFICIENTS $g_n(\beta)$ AND $h_n(\beta)$

n	$\beta=15^\circ$	30°	45°	60°	75°	$g_n(\beta)$	105°	120°	135°	150°	165°
1	.282143	.541363	.756806	.911554	.994212		.931349	.797843	.615545	.405599	.192216
2	-.084996	-.152410	-.186657	-.175962	-.113818		.158948	.349816	.553495	.746517	.903423
3	.022288	.039581	.047670	.043827	.027361		-.033885	-.067471	-.09470	-.095212	-.067787
4	-.002656	-.004763	-.005831	-.005488	-.003532		.004725	.009783	.013766	.014761	.010691
5	-.000371	-.000615	-.000653	-.000484	-.000206		-.000056	-.000474	-.001147	-.001700	-.001527
6	-.000350	-.000627	-.000768	-.000723	-.000465		.000618	.001272	.001772	.001874	.001332
7	.000471	.000831	.000991	.000900	.000552		-.000651	-.001249	-.001621	-.001596	-.001059
8	-.000083	-.000149	-.000181	-.000168	-.000111		.000146	.000300	.000369	.000438	.000311
9	-.000065	-.000112	-.000127	-.000110	-.000059		.000049	.000070	.000055	.000016	-.000013
10	-.000027	-.000049	-.000060	-.000059	-.000037		.000048	.000099	.000137	.000147	-.000100
11	.000097	.000179	.000225	.000215	.000141		-.000185	-.000373	-.000497	-.000498	-.000331
12	-.000011	-.000019	-.000024	-.000022	-.000015		.000019	.000038	.000053	.000057	.000041
13	-.000018	-.000030	-.000038	-.000033	-.000018		.000017	.000027	.000028	.000019	.000008
						$h_n(\beta)$					
0	.958946	.840992	.661122	.442207	.212099		-.167520	-.270250	-.297693	-.251004	-.143633
1	.282143	.541363	.756806	.911554	.994212		.931349	.797843	.615545	.405599	.192216
2	-.042498	-.076205	-.093328	-.087981	-.056909		.079474	.174908	.276747	.373258	.451711
3	.007429	.013194	.015890	.014609	.009120		-.011295	-.022490	-.030490	-.031737	-.022596
4	-.000664	-.001191	-.001458	-.001372	-.000883		.001181	.002446	.003441	.003690	.002673
5	-.000074	-.000123	-.000131	-.000097	-.000041		-.000011	-.000095	-.000229	.000340	.000305
6	-.000058	-.000104	-.000128	-.000120	-.000077		.000103	.000212	.000295	.000312	.000222
7	.000067	.000119	.000142	.000129	.000079		-.000093	-.000178	-.000231	-.000228	-.000151
8	-.000010	-.000018	-.000023	-.000021	-.000013		.000016	.000031	.000039	.000038	.000024
9	-.000007	-.000012	-.000014	-.000012	-.000007		.000007	.000011	.000012	.000010	-.000006